

Projectile angular distribution in He single ionization by proton impact as a function of the ejected-electron energy

V. D. Rodríguez*

Departamento de Física, Facultad de Ciencias Exactas y Naturales, Universidad de Buenos Aires, 1428 Buenos Aires, Argentina

R. O. Barrachina*

Comisión Nacional de Energía Atómica, Centro Atómico Bariloche e Instituto Balseiro, 8400 Bariloche, Argentina

(Received 7 July 1997)

In this paper we study the single ionization of helium atoms by the impact of protons at intermediate energies. We present a continuum-distorted-wave–eikonal-initial-state calculation of the cross section doubly differential in the projectile scattering angle and the ionized electron energy. The internuclear interaction is incorporated by means of an eikonal phase approximation. This calculation includes a full account of the final-state interactions among the three collision partners, showing a much better agreement with the recent experimental data of Schulz *et al.* than other first-order theories. We also discuss the appearance of different structures associated with the electron capture to the continuum process and the binary-encounter projectile-electron collision. [S1050-2947(97)07912-2]

PACS number(s): 34.50.Fa

I. INTRODUCTION

The scattering of the projectile in ion-atom collisions has been experimentally investigated for excitation and electron-capture processes during the past two decades. Let us mention, for instance, the remarkable observation of Thomas' peak in charge exchange collisions by Horsdal-Pedersen *et al.* [1] in 1983. However, experimental studies of ionization processes have been mainly devoted to total cross sections or to the energy and angular distributions of the ejected electrons (see, for instance, the review by Rudd *et al.* [2]).

The cross-section differential in the projectile scattering angle has been available only for a few years. The first experimental results concentrated on helium ionization by proton and deuteron impact at intermediate and high energies (0.1–6/amu) [3–6]. In the high-energy range (1–6 MeV/amu), a distinctive shoulder in the cross section was observed at a projectile scattering angle θ_p equal to m_e/M_p , where m_e and M_p are the electron and projectile masses, respectively [4]. This shoulder comes from the dominant contribution of the binary projectile-electron collision for θ_p smaller than this critical angle. This structure is fairly reproduced even by the simplest plane-wave Born approximation (PWBA) [4]. For angles larger than m_e/M_p , however, the binary collision mechanism does not hold, and the PWBA fails, dropping faster than the experimental results. At these larger scattering angles, the projectile deviation is mainly due to the interaction with the target core [7]. Later theoretical descriptions [7–11] did include both the projectile-electron and the internuclear interaction in order to get a correct description of the projectile deflection. In particular, the well-established continuum-distorted-wave–eikonal-

initial-state (CDW-EIS) theory [12,13], including both interactions, was compared in a recent paper [14] with the available projectile scattering measurements in proton-helium single ionization collisions [4,5]. This distorted-wave calculation was shown to give an improved description of the experimental data even at the lowest available impact energies (100–300 keV/amu).

In a recent work by Schulz *et al.* [15], doubly differential cross sections for $H^+ + He$ ionization collisions have been systematically measured as a function of the projectile energy loss and scattering angle in a lower energy range (50–150 keV). In principle, multiply differential cross sections display collision properties that are washed out by integration in total cross sections. Furthermore, they are more sensitive to deviations between experimental and theoretical results than integral cross sections. These data were compared with a first-order Born approximation ($B1$) which includes the target ion-electron interaction in the final state. A modified $B1$ calculation was also considered, where the final-state interaction of the electron with the receding projectile is partially taken into account by multiplying the $B1$ transition amplitude with the electron-projectile Coulomb normalization factor [16]. This *distortion* of the $B1$ approximation improves the comparison with the measured doubly differential cross section in the matching velocity region, i.e., when the electrons move at the same speed as the projectile. However, important discrepancies that were observed for large scattering angles were attributed to the fact that the projectile-target nucleus interaction was not included in either $B1$ approximation. Schulz *et al.* [15] also compared their experimental data with a classical trajectory Monte Carlo calculation, which exhibits a much better agreement for large scattering angles.

The objective of the present work is to compare these recent experimental data with a CDW-EIS calculation, including a full account of the final-state interactions among the three collision partners (electron, projectile, and residual target). The theory is briefly reviewed in the following sec-

*Also a member of the Consejo Nacional de Investigaciones Científicas y Técnicas (CONICET), Argentina.

tion. Since we are particularly interested in the projectile angular distribution, much care has been taken in the calculation to get a proper description of the internuclear interaction. These theoretical results are compared in Sec. III with the experimental data of Schulz *et al.* [15] and with other theoretical descriptions.

II. GENERAL THEORY

Let us consider the single ionization of a hydrogenic target of charge Z_T by the collision of a projectile of charge Z_P and velocity v_P . The outcome of this collision process may be described by the electron momentum \mathbf{k} and the direction Ω_P of the scattered projectile momentum \mathbf{K} . The corresponding quintuply differential cross section in the center-of-mass coordinate system reads (atomic units are used throughout)

$$\frac{d\sigma}{d\mathbf{k}d\Omega_P} = \frac{\mu^2}{4\pi^2} |T(\boldsymbol{\eta})|^2, \quad (1)$$

with $\mu = M_P(1 + M_T)/(1 + M_T + M_P)$ the reduced mass in the initial projectile-target configuration. $T(\boldsymbol{\eta})$ is the corresponding transition matrix element, with $\boldsymbol{\eta}$ the transversal component of the momentum $\mu\mathbf{v}_P - \mathbf{K}$ transferred in the collision. For small projectile scattering angles, $\boldsymbol{\eta} \approx \mu v_P \boldsymbol{\theta}_P$, with θ_P the projectile scattering angle. The transformation from the center-of-mass to the laboratory frame can be performed by replacing μ in Eq. (1) by the projectile mass M_P [7].

For a long time, most measurements of single-ionization collisions were restricted to the momentum distribution of the ejected electron, integrated over the projectile scattering angles

$$\frac{d\sigma}{d\mathbf{k}} = \int \frac{d\sigma}{d\mathbf{k}d\Omega_P} d\Omega_P. \quad (2)$$

However, some recent papers [4,5] have reported measurements of the projectile angular distribution

$$\frac{d\sigma}{d\theta_P} = 2\pi \sin\theta_P \int \frac{d\sigma}{d\mathbf{k}d\Omega_P} d\mathbf{k} \quad (3)$$

for the ionization of helium by high-energy proton and deuteron impact. The dependence on the polar angle ϕ_P vanishes because of the symmetry of the system.

Recent developments in coincidence techniques and cold-target recoil-ion spectroscopy [17,18] have also made it possible to measure higher differential cross sections with respect to practically any combination of the momenta of the three final-state particles. This is the case, for instance, of the cross section

$$\frac{d^2\sigma}{dE_e d\Omega_P} = \sqrt{2E_e} \int \frac{d\sigma}{d\mathbf{k}d\Omega_P} d^2\hat{\mathbf{k}}, \quad (4)$$

differential in the projectile scattering angle θ_P and the ionized electron energy $E_e = k^2/2$ (the dependence on ϕ_P vanishes). While some previous measurements only concentrate on some fixed scattering angles [19], in a recent experiment

by Schulz *et al.* [15] for 50–150 keV $H^+ + He$ single-ionization collisions, this doubly differential cross section has been systematically measured in a range of scattering angles (0–1.5 mrad) and electron energies (1–95 eV).

These experimental advances triggered similar theoretical studies of highly differential ionization cross sections, including the projectile or recoil target-ion momentum distribution. These cross sections have been calculated in the plane-wave [4], first-order Born [7], eikonal distorted-wave [10], continuum distorted-wave [14], and Glauber [11] approximations. Also, the classical trajectory Monte Carlo calculation [15,19] and a semiclassical approximation with classical hyperbolic projectile trajectories [9,20] have been employed.

While the deflection of the projectile at large angles is mainly determined by its interaction with the target nucleus, the binary collision with the emitted electron plays an important role at angles smaller than m_e/M_P , which corresponds to the maximum angle of deflection by a free electron. Measurements of the singly differential cross section $d\sigma/d\Omega_P$ for high-energy $H^+ + He$ collisions show a conspicuous shoulder at exactly this limit angle $m_e/M_P = 0.545$ mrad [4]. The plane-wave Born approximation reproduces this small-angle distribution, but fails at larger angles, dropping rapidly with the scattering angle just above the maximum binary-collision angle m_e/M_P . The first-order Born approximation of Salin [7] gets a better comparison over a wide angular range, due to the inclusion of an eikonal phase related to the Coulomb interaction between the projectile and the target-nucleus. However, the shoulder is not reproduced at 3 MeV. This failure was attributed to the slow convergence of the partial wave expansion employed by this author.

The internuclear interaction can be accounted for by means of an integral transformation [14]

$$T(\boldsymbol{\eta}) = \int I(\boldsymbol{\eta} - \boldsymbol{\eta}') \tilde{T}(\boldsymbol{\eta}') d^2\boldsymbol{\eta}', \quad (5)$$

where the *reduced* transition matrix element \tilde{T} is evaluated in an approximation with the target ion-projectile interaction completely removed. For small-angle scattering, this internuclear potential $V_{PT}(R)$ can be accounted for by means of an eikonal phase factor [7]

$$I(\boldsymbol{\eta} - \boldsymbol{\eta}') = \frac{1}{4\pi^2} \int \exp\left(-i \int_{-\infty}^{\infty} V_{PT}(R) dt\right) \times \exp[-i(\boldsymbol{\eta} - \boldsymbol{\eta}') \cdot \boldsymbol{\rho}] d^2\boldsymbol{\rho}, \quad (6)$$

where $R = \sqrt{\rho^2 + v_P^2 t^2}$. In principle, $V_{PT}(R)$ represents a ‘‘static’’ core potential which distorts the projectile trajectory [21,22]. Assuming a pure Coulomb interaction between the projectile and target residual ion, this *kernel* reads

$$I(\boldsymbol{\eta} - \boldsymbol{\eta}') = \frac{1}{4\pi^2} \int \rho^{2iZ_P Z_T^*/v_P} \exp[-i(\boldsymbol{\eta} - \boldsymbol{\eta}') \cdot \boldsymbol{\rho}] d^2\boldsymbol{\rho}, \quad (7)$$

where we introduce an effective charge Z_T^* to account for the screening of the target nucleus charge by the passive elec-

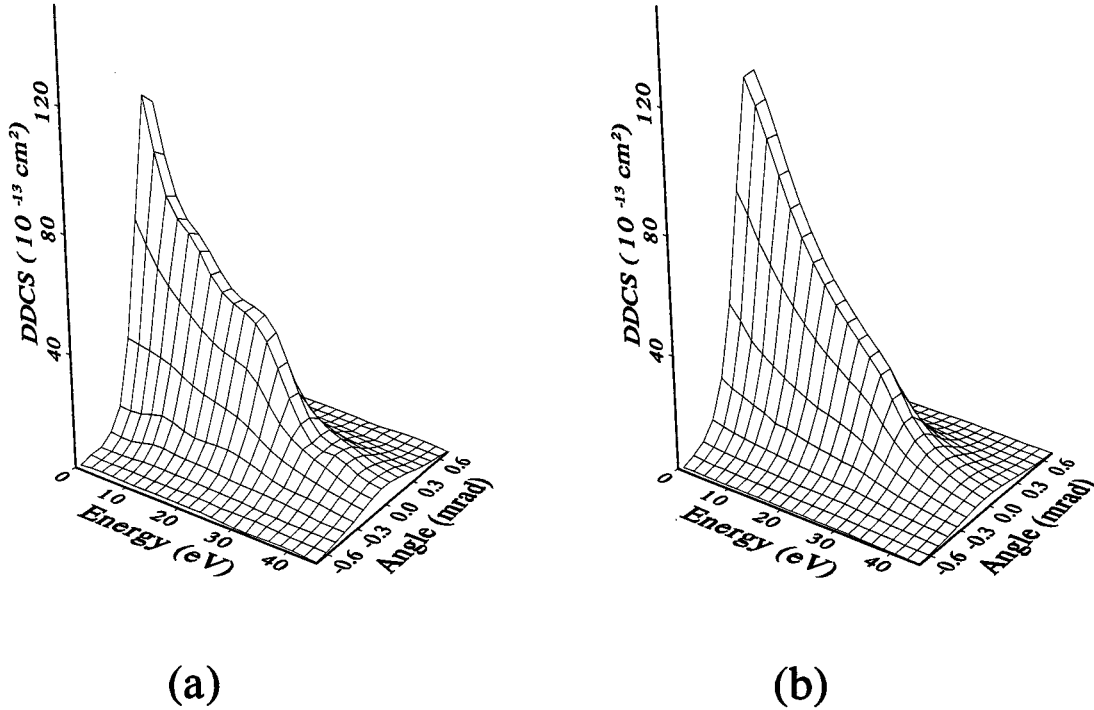


FIG. 1. (a) Doubly differential cross section for helium single-ionization at 50-keV proton impact as a function of the projectile scattering angle [15]. (b) CDW-EIS calculation.

tron. For helium we choose $Z_T^* = 1.35$, arising from the binding energy of the active electron.

For the reduced transition matrix element \tilde{T} in Eq. (5) we employ the CDW-EIS approximation, introduced by Crothers and McCann [12] for the ionization collision. While the initial scattering state is distorted by an eikonal phase factor for the electron-projectile Coulomb interaction, the final state incorporates the interaction of the emitted electron with both the projectile and the residual target ion, through a product of the individual Coulomb continuum wave functions ψ_{eP}^- and ψ_{eT}^- , respectively.

Here we want to calculate the reduced transition matrix element \tilde{T} in Eq. (5) for a single-ionization $H^+ + He$ collision. We employ an independent electron description of the two-electron target atom. The initial state is described by a Hartree-Fock wave function and the final state by a hydrogenic wave function with the effective charge Z_T^* [13]. The presence of two electrons in the target is taken into account by multiplying the corresponding single-ionization cross section by a factor two. We refer to the work by McCartney and Crothers [23] for an analytic expression of the reduced transition matrix \tilde{T} . The integral transformation in Eq. (5) is numerically performed as described in Ref. [14].

We want to point out that the CDW-EIS calculation incorporates the three interactions in the final state. It is only due to the large momentum of the projectile that the contribution of the internuclear potential can be singled out in an eikonal approximation as given in Eqs. (5) and (6). Since the kernel (6) verifies the following property:

$$\int I^*(\boldsymbol{\eta} - \boldsymbol{\eta}') I(\boldsymbol{\eta} - \boldsymbol{\eta}'') d^2 \boldsymbol{\eta} = \delta(\boldsymbol{\eta}' - \boldsymbol{\eta}''), \quad (8)$$

it is readily verified that the ionization cross section integrated in the projectile scattering angle can be calculated in terms of the reduced matrix element \tilde{T} alone, which is entirely independent of the internuclear potential,

$$\frac{d\sigma}{d\mathbf{k}} = \frac{\mu^2}{4\pi^2} \int |T(\boldsymbol{\eta})|^2 d^2 \boldsymbol{\eta} = 4\pi^2 \int |\tilde{T}(\boldsymbol{\eta})|^2 d^2 \boldsymbol{\eta}. \quad (9)$$

Thus, the internuclear interaction plays no sensible role in the momentum distribution of the emitted electron, and can be switched off in the corresponding calculation. However, this is not the case for the projectile emission angle distribution. In particular, a correct description of the deflection in angles larger than m_e/M_P can only be achieved through the interaction with the target nucleus.

III. COMPARISON WITH EXPERIMENTAL RESULTS

In what follows, cross sections and scattering angles are given in the laboratory system. In Fig. 1 we show three-dimensional plots of the doubly differential cross section (DDCS) $d^2\sigma/dE_e d\Omega_P$ for helium single-ionization at 50-keV proton impact. The experimental data of Schulz *et al.* [15] [Fig. 1(a)] are compared with the present CDW-EIS calculation [Fig. 1(b)]. We clearly see that the main features of the experimental cross section are reproduced by the CDW-EIS model. Both plots show a shoulder at an energy around $E_e = m_e v_p^2 / 2 = (m_e / M_P) E_P \approx 25$ eV, that corresponds to electrons moving at the same velocity than the projectile. This structure is a fingerprint of the well-known ‘‘electron capture to the continuum’’ cusp in the electron spectra [16,24,25]. We may note that at the forward direction, the theory underestimates the experimental data at en-

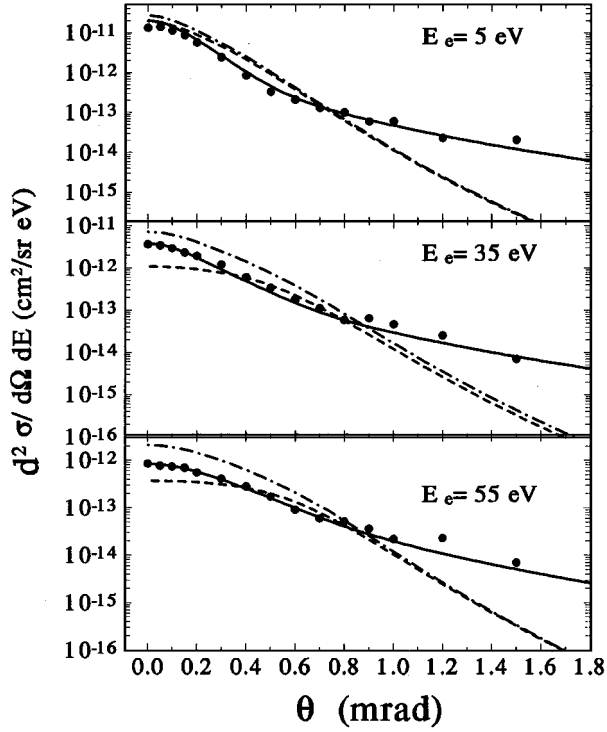


FIG. 2. Doubly differential cross section for helium single-ionization at 75-keV proton impact as a function of the projectile scattering angle for fixed values of the ionized electron energy E_e . The points are the experimental data of Schulz *et al.* [15]. The solid curve is the present CDW-EIS calculation. The dash-dotted and dashed lines represent the first Born approximation with and without electron-projectile Coulomb normalization factor, respectively [15].

ergies larger than E_e , so the shoulder is slightly less pronounced. We would like to point out that no normalization procedure has been carried out, and the actual z -axis units are shown in the figure.

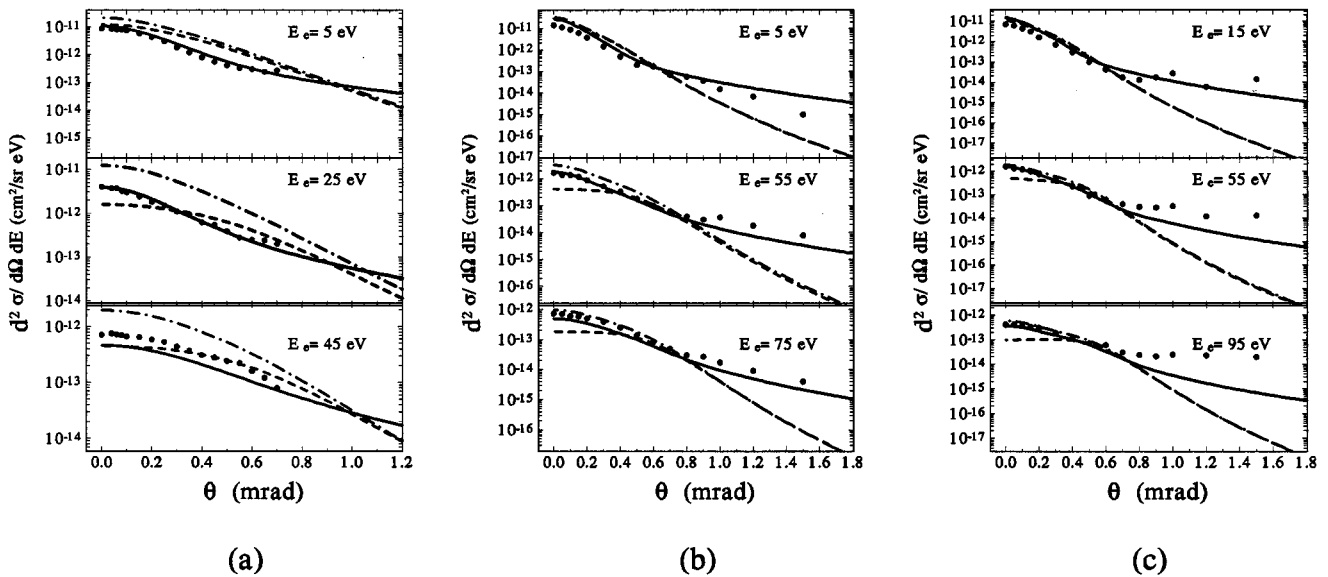


FIG. 3. Same as Fig. 2 but for 50, 100, and 150 keV.

In Fig. 2, we show these same experimental data and CDW-EIS calculation as function of the projectile scattering angle θ_p for fixed values of the ionized electron energy E_e . We note that the CDW-EIS doubly differential cross sections (solid line) agree well with the experimental data, both in magnitude and shape. On the other hand, both first Born ($B1$) calculations, with (dash-dotted line) and without (dashed line) the electron-projectile Coulomb normalization factor, show significant discrepancies, especially for large scattering angles where they underestimate the data. As it has been already mentioned, the reason for this failure is that the internuclear interaction is not explicitly included in these theories. Forcing the inclusion of the internuclear interaction in the $B1$ calculation [7] improves the agreement with the experimental data at large scattering angles, but leads to even worse results in the forward direction.

In Fig. 3 we show a similar comparison of experimental and theoretical results at proton energies of 50, 100, and 150 keV. As for the case shown in Fig. 2, we verify that the CDW-EIS calculation is in much better agreement with the experimental data than the other considered theories. At the lowest impact energy (50 keV), the theory underestimates the data for an electron energy of 45 eV, as noted before. For 100- and 150-keV proton impact energies, the global agreement is good. In particular, our theoretical results remain close to the experimental data at small and intermediate proton scattering angles. For 150 keV, the present CDW-EIS calculations underestimate the data at large scattering angles.

Classical trajectory Monte Carlo (CTMC) calculations [8,9] are not shown in the previous figures. We refer to the paper by Schulz *et al.* [15] for a comparison of their experimental data with the CTMC model. We would only mention that the agreement of this theory with the experimental results of Schulz *et al.* is as good as for the CDW-EIS calculation, with a similar failure at 50 keV. CTMC calculations for 75 keV impact energy has not been reported.

No characteristic structure (Bethe ridge) [26] related to the binary projectile-electron scattering is observed in

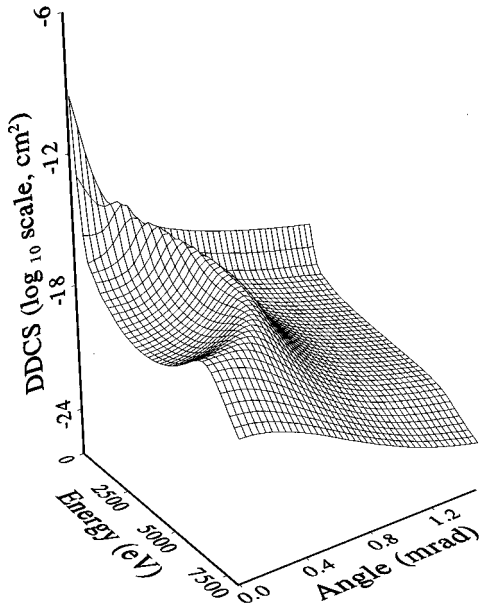


FIG. 4. CDW-EIS calculation of the doubly differential cross section for helium single-ionization at 3-MeV proton impact as a function of the projectile scattering angle θ_p and electron energy E_e .

$d^2\sigma/dE_e d\Omega_p$ in any of the previous figures. Such structure would only emerge at much larger impact energies (above 1 MeV), as a ridge in the doubly-differential cross section located at [14]

$$\theta_p \approx \frac{m_e}{M_p} \sqrt{4 \frac{E_e}{2m_e v_p^2} \left(1 - \frac{E_e}{2m_e v_p^2}\right)}. \quad (10)$$

The appearance of this ridge at large impact energies is exemplified in Fig. 4 by a CDW-EIS calculation of the doubly differential cross section $d^2\sigma/dE_e d\Omega_p$ for a 3 MeV $H^+ + He$ single-ionization collision. This structure is slightly smeared by the initial momentum distribution of the electron in the target. The recoiling electrons from those events contributing to the emergence of this structure form the binary-encounter ridge in the momentum distribution of the emitted electrons [27]. No measurements of the Bethe ridge have been re-

ported yet, although calculations with the Bethe approximation has been published [26]. In contrast to the present results, previous calculations show an exponential fall-off for angles larger than 0.8 mrad. This is the case because beyond the binary projectile-electron ridge, only the internuclear interaction may deflect the projectile. Therefore, theoretical calculations ignoring the internuclear interaction largely underestimate the tail of the cross sections, showing an exponential dependence, instead of the well-known Rutherford scattering behavior for large scattering angles.

IV. CONCLUSIONS

In the present work we have compared a CDW-EIS calculation of the doubly differential cross section $d^2\sigma/dE_e d\Omega_p$ for $H^+ + He$ single-ionization collisions with recent experimental data by Schulz *et al.* We showed that the CDW-EIS calculation reproduce the main features of the experimental cross section. For all the considered projectile energies (50, 75, 100, and 150 keV), the CDW-EIS calculation is in much better agreement with the experimental data, both in magnitude and shape, than other first-order theories. Here we have described the projectile-target core interaction by means of a pure Coulomb potential with an effective charge Z_T^* . Further improvements of the theory might be expected from the use of a static core potential $V_{pT}(R)$ showing the required Coulomb behavior with target-core charges Z_T and $Z_T - 1$ for close and distant collisions, respectively.

We conclude that the CDW-EIS approximation, including a full account of the final-state interactions among the three collision partners (electron, projectile, and residual target), seems to be a qualified theory for describing the projectile deflection in single-ionization ion-atom collisions.

ACKNOWLEDGMENTS

This work has been supported by the Consejo Nacional de Investigaciones Científicas y Técnicas under Contract No. PICT 0204/97-CONICET. V.D.R. acknowledges support by the Universidad de Buenos Aires under Project No. EX052/J-UBA. Instituto Balseiro is affiliated with the Universidad Nacional de Cuyo, Argentina.

[1] E. Horsdal-Pedersen, C. L. Cocke, and M. Stockli, Phys. Rev. Lett. **50**, 1910 (1983).
 [2] M. E. Rudd, Y.-K. Kim, D. H. Madison, and T. J. Gay, Rev. Mod. Phys. **64**, 441 (1992).
 [3] J. P. Giese and E. Horsdal, Phys. Rev. Lett. **60**, 2018 (1988).
 [4] E. Y. Kamber, C. L. Cocke, S. Cheng, J. H. McGuire, and S. L. Varghese, J. Phys. B **21**, L455 (1988); E. Y. Kamber, C. L. Cocke, S. Cheng, and S. L. Varghese, Phys. Rev. Lett. **60**, 2026 (1988).
 [5] F. G. Kristensen and E. Horsdal-Pedersen, J. Phys. B **23**, 4129 (1990).
 [6] A. Gensmantel, J. Ullrich, J. Dörner, and R. E. Olson, Phys. Rev. A **45**, 4572 (1991).

[7] A. Salin, J. Phys. B **22**, 3901 (1989).
 [8] R. E. Olson, J. Ullrich, R. Dörner, and H. Schmidt-Böcking, Phys. Rev. A **40**, 2843 (1989).
 [9] M. Horbatsch, J. Phys. B **22**, L639 (1989).
 [10] H. Fukuda, I. Shimamura, L. Végh, and T. Watanabe, Phys. Rev. A **44**, 1565 (1992).
 [11] X. Fang and J. F. Reading, Nucl. Instrum. Methods **53**, 453 (1991).
 [12] D. S. F. Crothers and J. F. McCann, J. Phys. B **16**, 3239 (1983).
 [13] P. D. Fainstein, V. H. Ponce, and R. D. Rivarola, J. Phys. B **24**, 3091 (1991).
 [14] V. D. Rodríguez, J. Phys. B **29**, 275 (1996).

- [15] M. Schulz, T. Vajnai, A. D. Gaus, W. Htwe, D. H. Madison, and R. E. Olson, *Phys. Rev. A* **54**, 2951 (1996).
- [16] A. Salin, *J. Phys. B* **2**, 631 (1969).
- [17] J. Ullrich, R. Dörner, V. Mergel, O. Jagutzki, L. Spielberger, and H. Schmidt-Böcking, *Comments At. Mol. Phys.* **30**, 285 (1994).
- [18] R. Dörner, V. Mergel, Liu Zhaoyuan, J. Ullrich, L. Spielberger, R. E. Olson, and H. Schmidt-Böcking, *J. Phys. B* **28**, 435 (1994).
- [19] G. Schiwietz, *Phys. Rev. A* **37**, 370 (1988).
- [20] D. Trautmann, F. Rösel, and G. Baur, *Nucl. Instrum. Methods Phys. Res. A* **232**, 218 (1984).
- [21] C. J. Joachain and R. Vanderpoorten, *J. Phys. B* **6**, 622 (1973).
- [22] R. D. Rivarola, R. D. Piacentini, A. Salin, and Dž. Belkić, *J. Phys. B* **13**, 2601 (1980).
- [23] M. McCartney and D. S. F. Crothers, *J. Phys. B* **26**, 4561 (1993).
- [24] G. B. Crooks and M. E. Rudd, *Phys. Rev. Lett.* **25**, 1599 (1970).
- [25] J. H. Macek, *Phys. Rev. A* **1**, 235 (1970).
- [26] M. Inokuti, *Rev. Mod. Phys.* **43**, 297 (1971).
- [27] D. H. Lee, P. Richard, T. J. M. Zouros, J. M. Sanders, J. L. Shinpaugh, and H. Hidmi, *Phys. Rev. A* **41**, 4816 (1990).